American Journal of Analytical Chemistry, 2024, 15, 72-98
https://www.scirp.org/journal/ajac
ISSN Online: 2156-8278
ISSN Print: 2156-8251

Interactions of Aurein with Model Membranes and Antimalarials

Anaif M. Alhewaitey[1,2], Nsoki Phambu[1], Naif M. Alhawiti[3]

[1]Department of Chemistry, Tennessee State University, Nashville, USA
[2]Department of Chemistry, University of Tabuk, Tabuk, Saudi Arabia
[3]CAHFS, University of California Davis, Davis, USA
Email: Dr.vet.naif@gmail.com

How to cite this paper: Alhewaitey, A.M., Phambu, N. and Alhawiti, N.M. (2024) Interactions of Aurein with Model Membranes and Antimalarials. *American Journal of Analytical Chemistry*, **15**, 72-98.
https://doi.org/10.4236/ajac.2024.152005

Received: January 5, 2024
Accepted: February 25, 2024
Published: February 28, 2024

Abstract

Aurein is a cationic antimicrobial peptide, rich in phenylalanine residues. Although the peptide has been extensively studied, its mechanism of action is not fully understood and has not been established. This project is focused on studying the interactions of aurein with model biological membranes and antimalarials using Fourier Transform Infrared (FTIR), fluorescence, dynamic light scattering (DLS), atomic force microscopy (AFM), thermogravimetric analysis (TGA), and differential scanning calorimetry (DSC) techniques. FTIR data revealed conformational changes to the secondary structure of the peptide in the presence of the model membranes. The strongest interactions of aurein were found with DOPC and lipid raft systems. Fluorescence data revealed some differences in the mechanism of interaction between aurein and lipid rafts. Topographical analysis was performed using atomic force microscopy (AFM). AFM images of the peptide with its lipid rafts showed a change in surface roughness suggesting a different mechanism of interaction. DLS data in agreement with FTIR confirmed that aurein interacts differently with the lipid rafts. The results gathered from this study provided new insights on the interaction of aurein. On the other hand, drug-drug interaction issues continue to present a major dilemma for the clinician caring for complex patients such as those infected with infectious disease. This study has examined the interaction of aurein with quinine, primaquine, and chloroquine. Significant interactions between aurein and antimalarials occured at a higher concentration of antimalarials. Interactions between aurein and antimalarials reveal a strong interaction between aurein and primaquine. Interactions between aurein and quinine or chloroquine were found to be weak and negligible. FTIR, TGA, and DSC may be used in a complementary way to gain insights into the possible drug-drug interactions involving aurein. These studies are needed to initiate *in vivo* controlled interaction studies between

antibiotics and antimalarials.

Keywords

Aurein, Fluorescence, DPPC, SPM, cholesterol, DPPC-SPM-CHOL, Quinine, Antimalarials

1. Introduction

Over the past several decades, there has been an unprecedented increase in the number of antibiotic-resistant strains of bacteria, which has posed serious threat to conventional antimicrobial therapies [1] [2]. As various "superbugs" continue to resist even the most potent drugs, the need to develop new classes of drugs has never been so urgent. Antimicrobial peptides are a special class of proteins that has found novel use as potential alternative therapeutic agents [1] [2] [3]. The novel mechanisms of action which need to be explored further, as well as the broad-spectrum antibacterial activity of AMPs, have revamped hope of overcoming drug resistance. Most AMPs are known to deploy some form of membrane disruption, which in essence, makes it very difficult for bacteria to develop resistance to AMPs [4] [5] [6]. Antimicrobial peptides are a group of proteins with low molecular weights, which exhibit broad spectrum activity against a wide range of disease-causing pathogens such as bacteria, fungi, and viruses. The number of amino acids present in different AMPs varies depending on the type of AMP [4] [7] [8]. Among the most widely studied AMPs is a novel class of peptides called aureins. The discovery of aurein 1.2 came about as a result of many years of study in which researchers succeeded in isolating about 33 aurein peptides from two species of Australian tree frog; 17 peptides from *Litoria aurea* and 16 peptides from *Litoria raniformis* [7] [8]. Aurein 1.2 is among the most active of all other peptides as depicted by its ability to display strong antimicrobial and anticancer activity. Its protein chain is comprised of 13 amino acid residues (GLFDIIKKIAESF-NH2) [9] [10]. Aurein 1.2 has been chosen in this study for several reasons. Aurein 1.2 is the smallest AMP to be isolated from an anuran with the ability to display anticancer and antibiotic activity [8] [9] [10]. Given its high antimicrobial activity, aurein 1.2 **Figure 1** can shed a lot of light regarding how antimicrobial peptides interact with lipid membranes of microbes leading to lysis and cell death. Cell membranes defined and types as lipids comprise a large group of molecules that occur naturally and are made up of hydrocarbons that give structure and function to living cells. Lipids can be classified into various types, namely storage lipids, structural lipids, and other lipids [11]-[16]. Fatty acids—These are the most abundant and functionally important lipids in cells they contribute significantly to the metabolic and structural properties of cells. Fatty acids are sourced from triacylglycerols as a source of energy during fasting [13] [15] [16]. Triacylglycerols—These are the main forms of stored

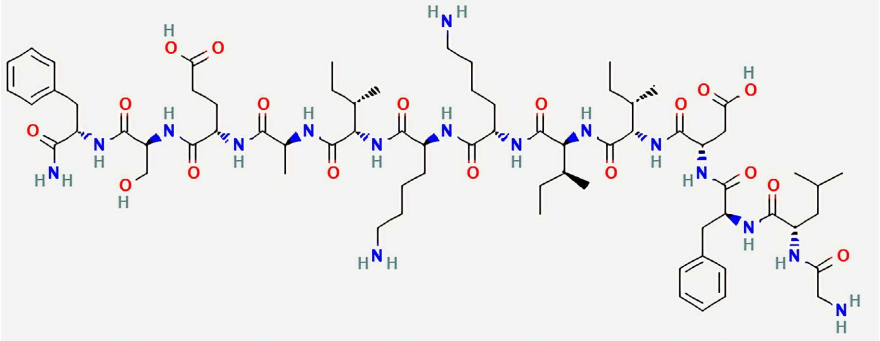

Figure 1. The molecular structure of Aurein 1.2.

fatty acids comprising of long hydrocarbon chains. Triacylglycerols are composed of a triester made up of three fatty acids and glycerol [13] [14]. Mono-, Di- and Tri-acylglycerols—The production of triacylglycerols involves the formation of intermediate molecules such as 1,2-Diacylglycerols which act as second messengers in various cellular processes. When triacylglycerols undergo digestion in the intestines, monoacylglycerols are formed [15] [16] [17]. Sterols-These lipids are found in almost all tissues, but their presence is mostly abundant in membranes [6] [11] [18]. Model Membranes, Phospholipids—These are subdivided into glycerolphospholipids and sphingolipids. The most abundant glycerolphospholipids are phosphatides, in which glycerol is replaced by 2 fatty acid esters [16] [17] [18] [19]. Phosphatides also contain three alcohols namely: serine, ethanolamine, and choline. Sphingolipids are composed of sphingoid base, which is attached to a fatty acid via an amide bond. In the tissues of animals, sphingomyelin is the predominant form of sphingolipids. Other lipids-These include lipoproteins, proteolipids, and polyketides [20]. These are structural phospholipids that contain the molecule choline as their headgroup [21]. They are a major constituent of biomembranes and can be extracted with ease from a variety of sources using mechanical or chemical means such as hexane. The sources of Dioleoylglycerophosphocholine DOPC and Dipalmitoylphosphocholine DPPC include soybeans and egg yolk, among other animal and plant tissues [21] [22] [23] [24]. In fact, all animal and plant cells contain phosphatidylcholines to which DOPC and DPPC belong [21] [23]. The structures of DPPC and DOPC are shown in **Figure 2** and **Figure 3**, respectively. The advantage of using DOPC and DPPC in cancer studies lies in their surface charge. Since cancer cells normally have altered physiology, their surface charge is also more anionic compared to healthy cells. As such, the use of anionic phospholipids DOPC and DPPC, which mimic phospholipids of cancer cells, enables one to study the interaction between the cationic AMP aurein 1.2 with these surface lipids [23] [24]. This concept is also important in terms of explaining the selective targeting of AMPs so that only cancerous cells are destroyed while healthy cells remain intact. Cholesterol is a type of lipid that helps to keep cell membranes firm and avoid becoming too fluid [13] [19]. It also helps control the permeability of cell

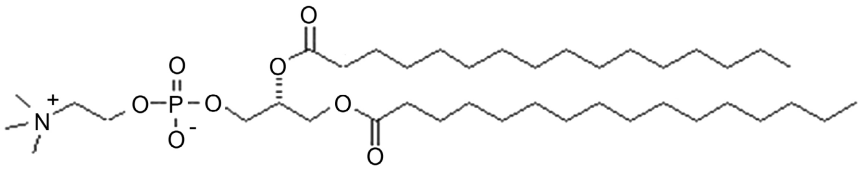

Figure 2. The molecular structure of DPPC.

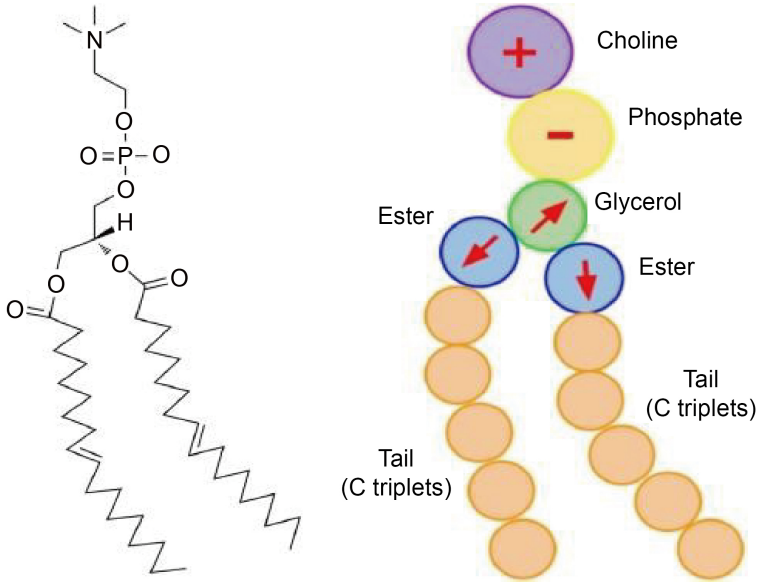

Figure 3. The molecular structure of DOPC lipid.

membranes by enhancing hospholipids packaging [16] [18]. Cholesterol can be extracted from a variety of sources such as egg yolk, meat, milk, and blood. Cholesterol (CHOL) is known as a "sterol" because it is made from alcohol and steroid. Cholesterol Figure 4 is in most animal membranes with varying amounts but is absent in prokaryotes and intracellular membranes, cholesterol is hydrophobic with molecular weight of 386.65 amu. Sphingomyelin (SPM) with molecular weight 646.505. Sphingomyelin Figure 5 is a kind of sphingolipid found in animal cell membranes, especially in the membranous myelin sheath that surrounds some nerve cellaxons. It usually contains phosphocholine and ceramide, or a phosphoethanolamine head group; therefore, sphingomyelins can also be classified as sphingophospholipids [18] [25] [26]. Statistically, drug reactions are ranked as between the 4th and 6th leading cause of death in the U.S. Prescription drugs can be used to effectively treat a vast variety of ailments. But with all of these different types of drugs, the potential for serious reactions to individual drugs, as well as the potential for dangerously combining certain drugs increases. The rise in deaths coincides with the direct marketing of prescription medication to the public.

Prescription drug sales have soared nearly 500 percent since 1990. With this increase of use, it becomes more important than ever to have an effective system for managing prescriptions to patients to help prevent drug interactions, serious

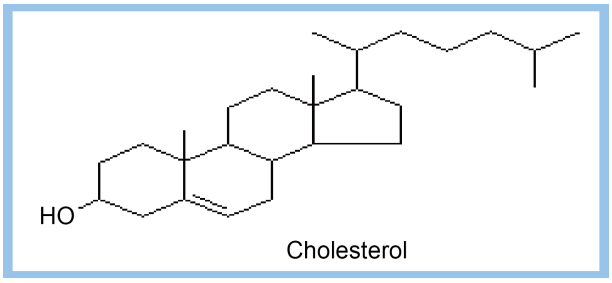

Figure 4. The molecular structure of cholesterol.

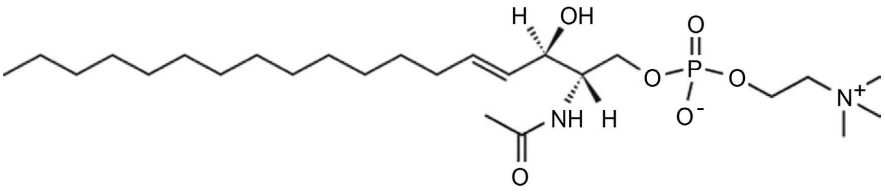

Figure 5. The molecular structure of SPM.

side effects, overdose, and death [27]. Malaria is one of the world's most common and serious tropical diseases, with half the world's population at risk of being infected with malaria. In addition, Malaria is among the diseases that has caused enormous losses to humankind since ancient times [28] [29]. Selected antimalarials, Quinine, also known as (8a,9*R*)-6'-Methoxycinchonan-9-ol is shown in **Figure 6**. Sources of Quinine include the barks of various trees such as cinchona, java, and Peruvian bark. Another natural source of Quinine is the bark of a flowering plant known as *Remijia*. The chemical structures of primaquine and chloroquine are presented in **Figure 7** and **Figure 8**. Chloroquine can be isolated from *Cassia sieberiana* as well as synthesized artificially [28] [29].

The objective of this paper is to investigate the mechanisms of interaction of the AMP aurein 1.2 with lipid raft model membranes (DOPC, DPPC, CHOL, and SPM) as well as with antimalarials (Quinine, Primaquine and Chloroquine) by various spectroscopic techniques.

2. Materials and Methods

2.1. Materials

2.1.1. Peptide Aurein

The peptide used in this study is aurein 1.2 with the amino acid sequence GLFDIIKKIAESF. It was purchased from GenScript as a white solid in 503.2mg vials with purity 97.3%. The peptide was used as it was received from the company without purification. It has a molecular weight of 1480.75 amu.

2.1.2. Water

Deionized water was obtained with Milli-Q A10 Synthesis machine by Millipore. A neutal pH was used for all interactions between antimicrobial peptide and model membranes; an acidic pH was used for all interactions between the antimicrobial peptide and antimalarials. To acidify water, HCl from Fisher was used

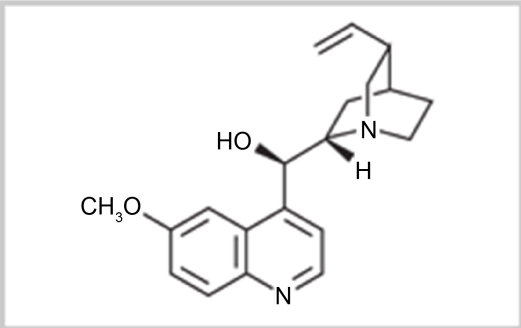

Figure 6. The molecular structure of Quinine.

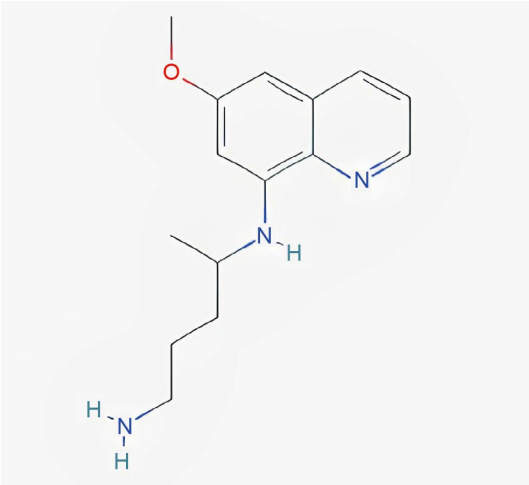

Figure 7. The molecular structure of Primaquine.

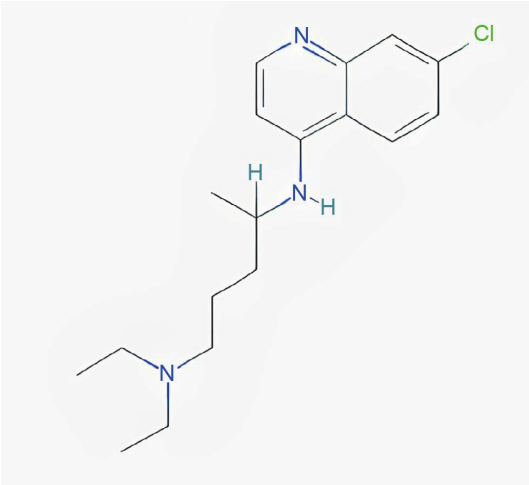

Figure 8. The molecular structure of Chloroquine.

as received.

2.1.3. Phospholipids

Phospholipids were purchased from Avanti Polar Inc and used as received. The phospholipids considered in this project are DPPC, DOPC, sphingomyelin and

cholesterol. 1,2-dipalmitoyl-sn-glycero-3-phosphatidylcholine (DPPC) a zwitterionic lipid with a molecular weight of 734.05 amu was used mimic the bulk of lipids in Eukaryotic membranes. 1-hexadecanoyl-2-(9Z-octadecenoyl)-sn-glycero-3-phosphocholin (POPC) the molecular weight of 760.076 amu. It was purchased from Avanti Polar Lipids. 1,2-Dioleoyl-sn-glycero-3-phosphocholine (DOPC) is a zwitterionic lipid with molecular weight of 786.113 amu and it was purchased from Avanti Polar Lipids.

2.1.4. Antimalarials

Antimalarials were purchased from Fisher and used as received. The most common antimalarials Quinine, Chloroquine diphosphate and Primaquine diphosphate were used in this project. Quinine, also known as (8a,9R)-6'-Methoxycinchonan-9-ol, with molecular weight 324.42amu. Chloroquine diphosphate with molecular weight 515.9 amu and Primaquine diphosphate with molecular weight 455.3 amu.

2.2. Methods

2.2.1. Preparation of Model Membrane and Antimalarials

We prepared solid and liquid samples of Phospholipids and antimalarials for different technics. A 4 mg of cholesterol with15mg of Aurein 1.2, 8 mg of each DOPC/DPPC with 15 mg of Aurein 1.2, and 7 mg of SPM with 15 mg of Aurein 1.2. 3 mg of Quinine with 15 mg of Aurein 1.2. 5 mg of each Primaquine diphosphate and Chloroquine diphosphate with 15 mg of Aurein 1.2. All these model membranes and antimalarials were prepared according to the literature. The list of peptide mixture:

- Aurein 1.2-DPPC
- Aurein 1.2-DOPC
- Aurein 1.2-CHOL
- Aurein 1.2-SPM
- Aurein 1.2-DPPC-CHOL-SPM
- Aurein 1.2-DOPC-CHOL-SPM
- Aurein 1.2-Quinine
- Aurein 1.2-Primaquine diphosphate
- Aurein 1.2-Chloroquine diphosphate

The model membranes and antimalarials were prepared going from large unilamellar vesicles (LUV) to small unilamellar vesicles (SUV). A vortex machine was used to ensure a homogenous mixture. Sonication of the resulting cloudy suspensions was done at 4˚C. The supernatant was decanted for immediate use. Lyophilization or freeze-drying makes the material more convenient for transport between −50˚C and −80˚C. Antimicrobial activity relates to the secondary and tertiary structure. Secondary structures of proteins include α-helices, β-sheets, β-turns, and random coils. Infrared, fluorescence, TGA, DSC, DLS and AFM were used to test the objective of this study [30] [31] [32]. IR was mainly used to determine the secondary structure of the peptide. The change in tertiary

structure was detected by Fluorescence. DLS was used to detect the size of the particles in liquid state, while AFM was used to detect the changes in surface roughness.

2.2.2. Infrared Concept

Infrared (IR) spectroscopy is widely used in both research and industry as a simple and reliable technique for measurement, quality control, and dynamic measurement of molecules [31] [32] [33]. It measures the changes in character or quantity of a particular bond at a specific frequency over time. For this study, this technique was used to measure the percent of secondary structure of the peptide (Aurein 1.2).

2.2.3. Curve Fitting Procedure

Determination of the secondary structure: curve fitting ATR IR studies of the amide I band of Aurein 1.2. For the determination of secondary structure from infrared spectra, Witold K. *et al*. [33] the determination of protein secondary the absorption of amino acid side chains show a matter of concern. This is because the amide I vibration of the polypeptide backbone used for this goal absorbs in a spectral region (1610 - 1700 cm^{-1}) where side chains also absorb. Thermo Fisher Scientific iS10 spectrometer was used to study the structure of the amide functional groups give rise to well-known signatures in the infrared region of the electromagnetic spectrum.

Determination of the secondary structure elements: curve fitting ATR IR studies of the amide I band of aurein. A curve fitting treatment was carried out to quantitatively estimate the relative proportion of each component representing a type of secondary structure. ATR FTIR (attenuated total reflectance Fourier Transform infrared) spectra of aurein and its complexes were recorded and used in this study. First, the IR spectra were normalized. Then a linear baseline was used between 1700 and 1600 cm^{-1}, and a FT Self-deconvolution was applied. The frequencies, the number of peaks to be fitted, and the half width (15 cm^{-1}) of each peak to start a least square iterative curve fitting procedure was obtained from the second derivative of the original IR spectra. Then the deconvolution of the amide I band was performed with OMNIC Software (Thermo Fisher Scientific, Waltham, MA), and analyzed as a sum of Gaussian curves, with consecutive optimization of amplitudes, band positions, half-widths, and Gaussian composition of individual bands. The amount of each secondary structure element is given in percentage terms, by dividing the area of one amide I band component by the area of the sum of all amide band component areas. **Table 1** shows the decomposition of Amide I Group with corresponding secondary structure.

2.2.4. Infrared Sample Preparation

Samples were prepared solid using a 1:1 molar ratio of peptide: peptide/phospholipid or antimalarial with 10^{-5} M molar concentration. Approximately 15 mg

Table 1. Decomposition of Amide I Group with corresponding secondary structure.

Secondary structure	Peak Number (cm^{-1})
Anti-β-sheets	1690 - 1699
Turns	1665 - 1690
α-helix	1648 - 1660
Randomcoils	1638 - 1647
β-sheets	1610 - 1637

of the peptide (Aurein 1.2) was dissolved in deionized water, for the phospholipid, 4 mg of the cholesterol, 8 mg for DOPC, 8 mg for DPPC, and 7 mg of SPM, 3mg of Quinine, 5 mg of Chloroquine diphosphate 5 mg of Primaquine were dissolved in deionized water.

A vortex machine was used to ensure a homogenous mixture. Sonication of the resulting cloudy suspensions was done then Lyophilization to dry the sample, which then become ready to use after one night.

2.2.5. Fluorescence

The Varian Cary Eclipse Fluorescence Spectrophotometer was used to obtain the data for fluorescence [34]-[43]. Fluorescence excites various select groups of molecular species, such as DNA, proteins, amino acids, coenzymes, pigments and dyes. The amino acids tyrosine, tryptophan and phenylalanine have an intrinsic fluorescence. For tyrosine and tryptophan, the excitation wavelength used is 275 nm and 280 nm, respectively. For phenylalanine, the excitation wavelength of 260 nm is used. Since (Aurein 1.2) contains Phenylalanine, it will be excited with the excitation wavelength of 260 nm. Samples in cuvettes were loaded into the sample chamber and excited at 260 nm. A spectrum obtained shows the intensity, wavelength and peak of the sample. Samples were prepared by mixing different amount of the peptide 5, 10, 15, 20, and 50 ml with 5 ml Aurein 1.2 phospholipids each time.

2.2.6. Differential Scanning Calorimetry (DSC)

Differential scanning calorimetry (DSC) is a thermoanalytical system in which the difference in the amount of heat required to increase the temperature of a sample and reference is measured as a function of temperature [30]. Both the sample and reference are kept up at about the same temperature throughout the experiment. For the most part, the temperature program for a DSC investigation is composed such that the sample holder temperature increases linearly as a function of time. The reference sample should have a well-defined heat capacity over the range of temperatures to be checked [35] [36] [37].

2.2.7. Dynamic Light Scattering (DLS): Particle Size Distribution

The size and distribution of aggregates in solution were measured by Dynamic Light Scattering using a Zetasiser Nano Series (Nano-ZS) instrument (Malvern Instruments, Malvern, UK) and a 633 nm laser diode. All measurements were

conducted at a scattering angle of 90˚. All samples were filtered, degassed and scanned using a 1-cm path length quartz cuvette. The samples were allowed to equilibrate for three minutes at 25˚C. The data were fitted using Malvern Instrument DTS software. These experiments were carried out at Vanderbilt (VINSE LAB).

2.2.8. Thermogravimetric Analysis (TGA) and Differential Scanning Calorimetry (DSC)

Thermal stability and phase transitions of aurein and its complexes were recorded by Thermogravimetric Analysis (TGA) and Differential Scanning Calorimetry (DSC) with a LINSEIS STA PT1600 instrument [38] [39]. This instrument determines simultaneous changes of mass and caloric reactions of a sample. The instrument performs tests from ultra-high vacuum 10^{-4} mbar to 5 bar over pressure. Samples weighing 10 - 15 mg were put in a ceramics pan, and an empty pan was used as a reference. Investigations were performed between 25 and 700˚C with a heating rate of 10˚C per minute. Transition parameters were obtained with incorporate software.

2.2.9. Atomic Force Microscopy

Atomic Force Microscopy (AFM) is a non-destructive method used widely to analyze various materials and surfaces [40] [41]. It is a scanning probe microscopy technique that employs the force between a probe and sample to provide images of its surfaces with nanoscale resolution. The nanostructures formed by self-assembly of the peptide in pure water (pH 3.8) in absence and presence of lipids were characterized by AFM. Approximately 15 µL of sample solution was placed on the surface of a freshly cleaved mica sheet fixed to a steel AFM sample plate. The sample was then allowed to settle for 30 minutes to allow the peptide/membrane to adhere onto the mica surface. It was then rinsed with 100 µL of pure water to remove any unattached peptides and salt components before being air-dried for four hours. All the AFM experiments carried out in this project were recorded using the tapping mode, with a Nanoscope V system (Brucker, USA) at Xavier University in New Orleans.

3. Results and Discussion

3.1. Infrared

FTIR spectroscopy was used to (a) monitor the conformation of Aurein in the dry state, both in the presence and absence of phospholipids, and to (b) locate the presence of Aurein within the phospholipid. Knowing the conformation of Aurein with and without the lipid is important because the activity of AMPs is directly related to the conformation [30] [31] [32] [33]. Most cationic AMPs have been found to use the helical structure to disrupt the cell membrane. In the presence of the lipid, FTIR allows us to observe the bands of the C=O and PO_2^- groups and phospholipid acyl chains to help determine the manner in which the aurein-lipid interaction may alter membrane integrity. Because the IR bands of

the amide I groups are so broad; we used the curve-fitting procedure to calculate the secondary structure elements (as described in the Materials and Methods section).

The results obtained for all the IR spectra of aurein-complexes, aurein-lipid rafts, and pure lipids are summarized in Tables 2-4, respectively. The results of the IR curvefitting curves of Aurein and its complexes are summarized in Table 5.

Table 2. Wave numbers characteristic of the main functional groups of aurein with its complexes.

Assignment	Wave number (cm^{-1})	Aurein	Aurein-SPM	Aurein-CHOL	Aurein-DOPC	Aurein-DPPC
OH/NH	3400 - 3100	3280	3283	3278	3280	3290
C-H	3100 - 2800	3059:2955	2920:2852	2942	2920:2855	2919:2854
C=O	1800 - 1700	1723			1731	1728
Amide I	1700 - 1600	1648	1651	1646	1654	1652
Amide II	1600 - 1500	1535	1537	1534	1540	1537
Amide III	1350 - 1250			1274		
Phosphate	1260 - 1050		1194		1198	1184
NH_4^+	1000 - 700		970:702		970	972:706

Table 3. Wave numbers characteristic of the main functional groups of aurein with its lipid rafts.

Assignment	Wave number (cm^{-1})	Aurein	Aurein-SPM-CHOL-DOPC	Aurein-SPM-CHOL-DPPC
OH/NH	3400 - 3100	3280	3293	3291
C-H	3100 - 2800	3059:2955	2925:2855	2918:2851
C=O	1800 - 1700		1729	1730
Amide I	1700 - 1600	1646	1653	1654
Amide II	1600 - 1500	1533	1539	1541
Amide III	1350 - 1250			
Phosphate	1260 - 1050		1198:1134:1057	1175:1051
NH_4^+	1000 - 700		970:701	972

Table 4. Wave number characteristic of the main functional groups of pure lipids.

Assignment	Wave number (cm^{-1})	DPPC	DOPC	SPM	CHOL
OH/NH	3400 - 3100	3355	3393	3292	3425
C-H	3100 - 2800	2956:2917:2849	3005:2922:2853	2918:2850	2931:2901:2867:2849
C=O	1800 - 1700	1733	1737		
Amide I	1700 - 1600				
Amide II	1600 - 1500				
Amide III	1350 - 1250				
Phosphate	1260 - 1050	1243:1198:1062	1242:1172:1090:1051	1237:1089:1054	1055
NH_4^+	1000 - 700	969:721	971:873:823:722	960:721	953:841 : 800:743

3.1.1. Infrared spectrum of Aurein

The IR spectrum of Aurein alone. In the 3300 - 2800 cm^{-1} region, Aurein presents bands at 3280 cm^{-1} that can be attributed to N-H groups, and bands at 3059 and 2955 cm^{-1} can be assigned to C-H groups. In the 1800 -1500 cm^{-1} region, aurein also presents bands at 1646 and 1533 cm^{-1} that are assigned to amide I and amide II vibrations, respectively. The amide I band is mostly represented by the C=O portion of the amide group, while the amide II band is mostly represented by the N-H portion of the amide group [42] [43] [44] [45]. The band at 1646 cm^{-1} is so broad that we used the curve-fitting procedure to calculate the sub elements. The IR curve-fitting results of the amide I group of Aurein presence of one peak at 1723 cm^{-1} (C=O), one peak at 1648 cm^{-1}, which is characteristic of an α-helix conformation (100%). The amide II group is represented by one peak at 1535 cm^{-1} [43] [44] [45] [46].

3.1.2. IR Spectra of Pure Lipids

IR spectra of DPPC, DOPC, Sphingomyelin (SPM), and Cholesterol. The results of all the IR spectra of pure lipids, including the most common lipids, DPPC and DOPC, are summarized in **Table 4**. The bands corresponding to the main functional groups (N-H, C-H, C=O, phosphate, and ammonium) are well described.

3.1.3. IR Spectra of the Interaction between Aurein and Its Complexes

We used the data of **Tables 2-5** to analyze how Aurein is interacting with each of the model membranes.

3.1.4. Summary of FTIR Results IR Spectra of Aurein and DPPC

Table 5 illustrates how the conformation of aurein slightly changed in the presence of DPPC. The content of α-helix is maintained. The C=O peak of aurein at 1723 cm^{-1} is shifted towards the higher wave number of 1728 cm^{-1}. The shift towards this higher wave number indicates weakening of the H bonds. The peak attributed to phosphate groups in DPPC **Table 4** shifted from 1198 cm^{-1} in DPPC to 1184 cm^{-1} in AUREIN-DPPC. Again, the shift of the phosphate group to lower wave number indicates a strong bond. The band of the C=O group at 1733 in DPPC shifts to 1728 cm^{-1} in aurein-DPPC complex. In summary, aurein

Table 5. IR curve-fitting results of aurein and its complexes.

Assignment	Aurein	Aurein-DPPC	Aurein-DOPC	Aurein-SPM	Aurein-CHOL	Aurein-CHOL-DOPC-SPM	Aurein-CHOL-DPPC-SPM
Helix	100%	100%	100%	64%	100%	53%	55%
Sheets				36%		128%	45%
Turns						19%	
Randon Coils							

interacts with DPPC through the C=O and phosphate groups. The ammonium group may also be involved in the bonding. It can also be noted that the acyl chain groups of DPPC are also involved in the interaction, as the wave number assigned to the acyl chains in the region 3100 - 2800 cm^{-1} are changed.

3.1.5. IR Spectra of Aurein and DOPC

We notice from Table 5 that the conformation of aurein has not changed in the presence of DOPC. The C=O peak of aurein at 1723 cm^{-1} is shifted towards the higher wave number of 1731 cm^{-1} in aurein-DOPC complex. The shift towards this higher wave number indicates weakening of the H bonds. The peak attributed to phosphate groups in DOPC Table 4 shifted from 1172 cm^{-1} in DOPC to 1198 cm^{-1} in AUREIN-DOPC. Again, the shift of the phosphate group to higher wave number indicates a weak bond. The band of the C=O group at 1737 in DOPC shifts to 1731 cm^{-1} in aurein-DPPC complex. In summary, aurein interacts with DOPC through the C=O group. The ammonium group may also be involved in the bonding. It can also be noted that the acyl chain groups of DOPC are also involved in the interaction, as the wave number assigned to the acyl chains in the region 3100 - 2800 cm^{-1} are changed.

3.1.6. IR spectra of Aurein and SPM

It can be seen in Table 5 that the conformation of aurein changes slightly in the presence of SPM. There is a decrease in the content of α-helix, from 100% in the free aurein to 64% in aurein-SPM, and an appearance of β-sheets (36%). The C=O peak of aurein at 1723 cm^{-1} has disappeared, which suggests a strengthening of the hydrogen-bonds. The peak attributed to phosphate groups in SPM Table 4 at 1089 cm^{-1} in SPM is shifted to a higher wave number 1194 cm^{-1} in aurein-SPM. In summary, aurein interacts with SPM through a conformational change. The ammonium group may also be involved in the bonding. The acyl chain groups of SPM are changed.

3.1.7. IR Spectra of Aurein and Cholesterol

Table 5 illustrates how the conformation of aurein did not change in the presence of CHOL. The content of α-helix is maintained. The C=O peak of aurein at 1723 cm^{-1} has disappeared, which suggests a strengthening of the hydrogen-bonds. The peak attributed to phosphate groups in CHOL Table 4 has disappeared, which suggests a strong interaction.

In summary, aurein interacts with CHOL probably through the C=O and phosphate groups. This is suggested by the shift of the C-H bands of CHOL from 3425 cm^{-1} to 3278 cm^{-1} in aurein-CHOL. This large shift towards lower wavenumber is also an indication of strong interaction involving N-H groups. Aurein interacts with CHOL through N-H groups.

3.1.8. IR spectra of Aurein and DPPC-CHOL-SPM

Table 5 shows that the conformation of aurein completely changes in the pres-

ence of DPPC-SMP-CHOL. There is a decrease of the α-helical structure from 100% in free aurein to 55% in the lipid raft and an appearance of β-sheets (45%). The C=O peak of Aurein at 1723 cm^{-1} is shifted towards a higher wave number of 1730 cm^{-1}. The shift towards higher wave number indicates a weakening of the H bonds. The conclusion is aurein interacts with DPPC-SMP-CHOL through a conformational change.

3.1.9. IR Spectra of Aurein and DOPC-CHOL-SPM

Table 5 shows that the conformation of aurein completely changes in the presence of DPPC-SMP-CHOL. There is a decrease of the α-helical structure from 100% in free aurein to 53% in the lipid raft, an appearance of β-sheets (45%) and turns (19%). The C=O peak of Aurein at 1723 cm^{-1} is shifted towards a higher wave number of 1729 cm^{-1}. The shift towards higher wave number indicates a weakening of the H bonds. The conclusion is aurein interacts with DOPC-SMP-CHOL through a conformational change.

From the IR results, it can be stated that a strong interaction between aurein and the single model membranes occurs through a change in conformation (except for SPM) and the carbonyl, phosphate, acyl chains and ammonium groups are relatively involved. The mechanism of interaction between aurein and lipid rafts is different, as some turns structures appear in aurein-CHOL-DOPC-SPM. But these interactions of aurein with lipid rafts are very complex, as shown by the complexity of their FTIR spectra. Other techniques are needed to gain more insights into the mechanism of interaction.

3.2. Fluorescence

The phenylalanine emission fluorescence spectra of aurein with the single model membranes have given interesting results, which are listed in Tables 6-11. The molar ratios used for the complexes in Tables 6-8 are 1:1. Figure 9 displays the fluorescence emission of Aurein [40] [47] [48] [49]. Aurein in solution reveals two peaks, a small one at 284 nm with an intensity of 4, and a more intense peak at 307 nm, with an intensity of 18 a.u.

Table 6. Fluorescence data of aurein and its complexes with DPPC.

10^{-5} M DPPC	Peak (nm)	Intensity (a.u.)	Peak (nm)	Intensity (a.u.)	Peak (nm)	Intensity (a.u.)
0 mL	284.5	3.9	308.8	18		
1 mL	285.2	4	306.9	16.8		
2 mL	286	4.3	307	16.5	457	28.3
5 mL	285.4	3.2	307.1	9.7		
10 mL	285.4	3.2	308.6	5.8	421	0.3
15 mL	284.5	3.2	309	5.6	424.5	0.55
20 mL	286.5	2.9	306.9	4.2	424.1	0.39
50 mL	286.5	2.8	309.4	1.9	425.4	3

Table 7. Fluorescence data of aurein and its complexes with spm.

10^{-5} M SPM	Peak (nm)	Intensity (a.u.)	Peak (nm)	Intensity (a.u.)	Peak (nm)	Intensity (a.u.)
0 mL	286.2	3.8	306.8	18		
1 mL	285.9	4	308.2	15.9		
2 mL	285.6	3.5	306.8	13.1		
5 mL	284.8	3.6	307	8.9		
10 mL	284.5	3.5	308.6	5.7	422.7	0.58
15 mL	283.9	3.7	307.7	5.1	421.9	0.87
20 mL	284	3.2	306.9	4	422.8	1.17
50 mL	286.5	3.37	309.4	2.2	426.6	0.67

Table 8. Fluorescence data of aurein and its complexes with cholesterol.

10^{-5} M Aurein	10^{-5} M Cholester	Peak (nm)	Intensity (a.u.)	Peak (nm)	Intensity (a.u.)	Peak (nm)	Intensity (a.u.)
5 mL	0 mL	284.2	4.1	306.2	14		
5 mL	1 mL	285	4	305	17.3		
5 mL	2 mL	285	4	306	14.1		
5 mL	5 mL	284.2		307.1	11		
5 mL	10 mL	285	3.3	308	5.3		
5 mL	15 mL	285.4	3.3	307	6	422	0.6
5 mL	20 mL	285.2	3.1	309.4	4.2	423	1
5 mL	50 mL	285.2	3	313.3	2.3	425	0.5

Table 9. Fluorescence data of aurein and its complexes with cholesterol.

10^{-5} M Aurein 1.2	10^{-5} M Cholesterol	Peak (nm)	Intensity (a.u.)	Peak (nm)	Intensity (a.u.)	Peak (nm)	Intensity (a.u.)
5 mL	0 mL	284.2	4.1	306.2	14		
5 mL	1 mL	285	4	305	17.3		
5 mL	2 mL	285	4	306	14.1		
5 mL	5 mL	284.2		307.1	11		
5 mL	10 mL	285	3.3	308	5.3		
5 mL	15 mL	285.4	3.3	307	6	422	0.6
5 mL	20 mL	285.2	3.1	309.4	4.2	423	1
5 mL	50 mL	285.2	3	313.3	2.3	425	0.5

Table 10. Fluorescence data of aurein and its complexes with dppc-spm-chol.

Intensity (a.u.)	Peak (nm)	Intensity (a.u.)	Peak (nm)	Intensity (a.u.)	Peak (nm)	Intensity (a.u.)
4	306.4	18.3				
4	306.3	13.7				
3.5	307.9	9.9	400.7	0,97	423	0.35
3.2	309.4	4.1	424.8	0.4		
3	306	2.7	426.2	0.46		
2.7	309.4	2.46	421.9	0.5	155.4	0.29
3.2	309.4	1.8	422.8	0.9		
3	320.9	1.28	421.5	0.9	150.8	0.5

Table 11. Fluorescence data of aurein and its complexes with dopc-spm-chol.

Peak (nm)	Intensity (a.u.)	Peak (nm)	Intensity (a.u.)	Peak (nm)	Intensity (a.u.)	Peak (nm)	Intensity (a.u.)
285.7	4.2	307.6	18.7				
285.2	3.8	305.6	13.3				
284.5	3.5	304.6	9.4	442	1.15		
284.8	3.3	307.1	4.3	422	0.5		
284.5	3.1	309.4	2.8	422.7	0.48		
283.7	3.5	312	2.7	421.9	0.47	450.8	0.4
284	3.2	310.7	3.4	424.1	0.5	445.7	0.4
285.2	3.2	315.8	1.3	354	0.8	425.4	0.78

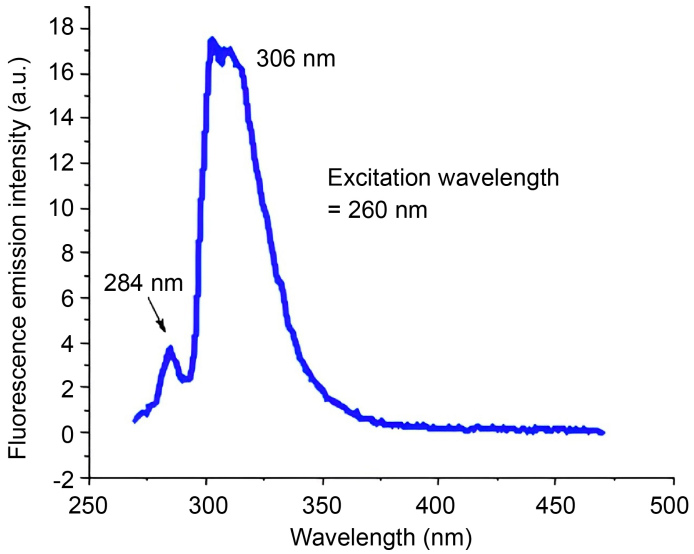

Figure 9. Fluorescence emission spectrum of aurein (excitation wavelength of 260 nm).

We monitored the main peak at 306 nm because it is more intense. Figure 10 shows how the peak at 306 nm varies with increasing amount of the selected model membrane DPPC-CHOL-SPM. The results of fluorescence data of aurein with its complexes are summarized in Tables 6-11. In the presence of model membranes, the fluorescence emission intensities of all the selected model membranes decrease significantly. This suggests a strong association between aurein and various lipids. The most significant decrease was found in the presence of DOPC. Interaction of aurein with cholesterol is weak Table 11. A specific experiment was performed to gain more insights into the effect of aurein on the model membranes DPPC-SMP-CHOL and DOPC-SPM-CHOL.

In the presence of the two systems, a decrease in emission intensity with a slightly red shift is observed. Overall, the interaction between aurein and model membranes seems to be stronger with DOPC, DPPC-SMP-CHOL, and DOPC-SPM-CHOL. The mechanism of interaction between aurein and the two lipid raft systems seems to be similar, as they lost the same amount of intensity.

3.3. DLS titration of Lipids with Aurein

To investigate the interaction of aurein lipid rafts, the effect on the size of a model membrane liposome with a specified amount of aurein was monitored [49]. The results of DLS data of aurein with its lipid rafts are summarized in the Table 12. The molar ratio between the model membranes and aurein is 1:1:1:1. The particle size of free aurein is 209 nm. In the presence of lipid rafts, the hydrodynamic radii decrease significantly. The size of the particle of aurein-DPPC-SPM-CHOL decreased from 209 nm to 176 nm (40% decrease), while that of

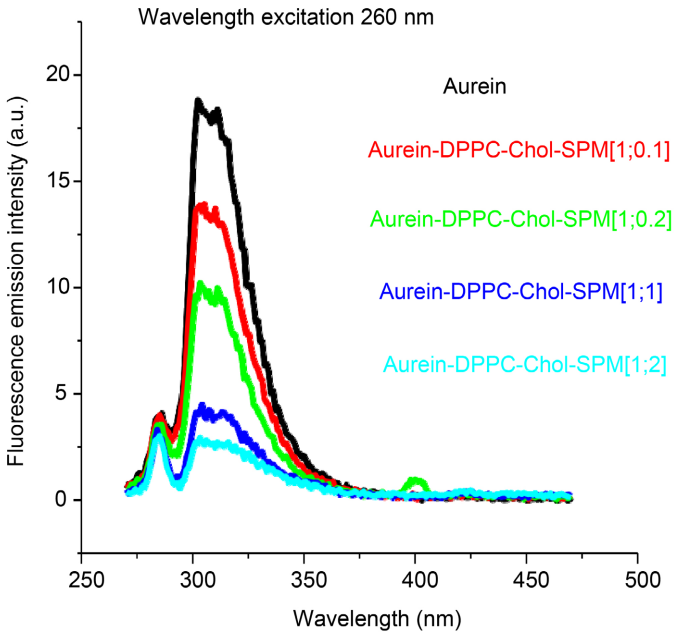

Figure 10. Fluorescence emission spectrum of aurein-DPPC-CHOL-SPM (excitation wavelength of 260 nm).

Table 12. Fluorescence data of aurein and its complexes using a peptide/lipidmolarratio of one to one.

Sample	[Peptide]/[membrane] Molar ratio	Wavelength (nm)	Intensity (a.u.)
Aurein	Freepeptide	306	18
Aurein-DPPC	1:1	307	10
Aurein-DOPC	1:1	309	4
Aurein-CHOL	1:1	307	11
Aurein-SPM	1:1	307	9
Aurein-DPPC/SPM/CHOL	1:1:1:1	309	4
Aurein-DPPC/SPM/CHOL	1:1:1:1	307	4

aurein-DOPC-SPM-CHOL decreased from 209 nm to 79 nm (62% decrease). Overall, the interaction between aurein and lipid rafts seems to be strong, but the mechanism of interaction may be different.

3.4. Atomic Force Microscopy

Morphological modifications induced by binding lipid rafts to aurein were examined by AFM [43] [44] [45]. Surface alterations are measured by the surface roughness by depositing prepared membranes onto mica substrates.

The research presents the AFM images of aurein and its complexes with lipid rafts. The results of AFM data of aurein with its lipid rafts are summarized in Table 13. The surface roughness of free aurein is 2.95 nm. In the presence of lipid rafts, the surface roughness changed. The surface roughness of aurein-DOPC-SPM-CHOL decreased from 2.95 nm to 1.13 nm, while that of aurein-DPPC-SPM-CHOL increased from 2.95 nm to 3.9 nm. The interaction between aurein and DOPC-SPM-CHOL is different with DPPCSPM-CHOL as evidenced by the values of roughness as seen in the AFM images.

3.5. Drug Interactions Aurein-Antimalarials

Interaction between drug substances may yield excessive risk of adverse drug reactions (ADRs) when two drugs are taken in combination. In this project, we examine the interactions of aurein with antimalarials using FTIR, TGA and DSC techniques.

3.5.1. Infrared

FTIR spectroscopy was used to monitor the conformation of aurein in the dry state, both in the presence and absence of antimalarials. FTIR was also used to identify the amin functional groups of Quinine, Primaquine and Chloroquine with and without aurein. The results obtained for all the IR spectra of aurein, Quinine, Primaquine, and Chloroquine, and their complexes are summarized in Table 14. The results of the IR curve-fitting curves of aurein and its complexes are summarized in Table 15.

Table 13. DLS data of aurein and the lipid rafts. The molar ratio between aurein and the lipid rafts is 1:1:1:1.

	Aurein	Aurein-chol/DPPC/SPM	Aurein-chol/DOPC/SPM
Hydrodynamic radius (nm)	209	126	79

Table 14. Roughness values of the AFM images obtained using tapping mode.

	Aurein	SPM-CHOL-DPPC	SPM-CHOL-DOPC	Aurein-SPM-CHOL-DPPC	Aurein-SPM-CHOL-DOPC
Roughness (nm)	2.95	2.04	5.23	3.9	1.13

Table 15. Wave numbers characteristic of the main functional groups of aurein and its complexes of antimalarials.

Assignment	Wave number (cm^{-1})	Aurein	Aurein-Quinine	Aurein-Chloroquin	Aurein-Primaquine
OH/NH	3400 - 3100	3280	3272	3271	3271
C-H	3100 - 2800	3059:2955	3067:2933	3032:2962:2877	3058
C=O	1800 - 1700		1726	1725	1730
Amide I	1700 - 1600	1646	1625	1624	1624
Amide II	1600 - 1500	1533	1534	1534	1531
Amide III	1350 - 1250				
Phosphate	1260 - 1050				
NH_4^+	1000 - 700				

The IR spectrum of aurein was described in the previous section. We focused on the FTIR spectra of the antimalarials. We used the data of Table 15 and Table 16 to analyze how aurein interact with each of the antimalarials.

1) IR spectra of aurein and Quinine

Table 14 and Table 15 illustrate how the conformation of aurein changed in the presence of Quinine. There is a decrease in the content of α-helix, from 100% in the free aurein, to 37% in aurein-Quinine; however, there is an increase in β-sheets from 0% to 49% in aurein-Quinine. The amide II group is split into two bands at 1543 cm^{-1} (59%) and 1517 cm^{-1} (41%). The C=O peak of aurein at 1723 cm^{-1} is shifted towards the higher wave number of 1729 cm^{-1}. The shift towards this higher wave number indicates weakening of the H bonds. In summary, aurein interacts with Quinine through a conformational change, and the N-H group of the amide II is involved in the bonding. It can also be noted that the C-H groups of Quinine are involved in the interaction, as the wave number assigned to the C-H in the region 3100 - 2800 cm^{-1} are changed.

2) IR spectra of aurein with Primaquine

We notice from Table 15 that the conformation of aurein has changed in the presence of Primaquine. There is a disappearance of the content of helix in aurein-Primaquine. All the helix content is converted to sheets (29%), turns (30%) and random coils (41%). The amide II group remains unchanged. In summary, aurein interacts with Primaquine through a conformational change,

Table 16. IR curve-fitting results of aurein and its complexes with antimalarials.

	Aurein	Aurein/Quinine	Aurein/Primaquine	Aurein/Chloroquine
a-Helix	100%	37%		34%
B-Sheet		49%	29%	56%
B-Turn		14%	30%	10%
Random Coil			41%	

and the N-H group of the amide group is involved in the bonding as their corresponding peak shifts from 3280 cm^{-1} to 3270 cm^{-1} in aurein-Primaquine. The C-H groups of Primaquine seem to be unchanged in the region 3100 - 2800 cm^{-1}.

3) IR spectra of aurein and Chloroquine

Table 15 indicates that the conformation of aurein changes in the presence of Chloroquine. There is a decrease in the content of α-helix, from 100% in the free aurein to 34% in aurein-Chloroquine, but an increase in β-sheets from 0% to 56% in aurein-Chloroquine. The amide II group remains unchanged. The C=O peak of aurein at 1723 cm^{-1} is shifted towards a higher wavenumber of 1727 cm^{-1}. The shift towards higher wavenumber indicates a weakening of the H bonds. In summary, aurein interacts with Chloroquine through a conformational change, and the N-H groups of the amide group are involved in the bonding.

From the IR results, it can be stated that a strong interaction between aurein and antimalarials occurs through a change in conformation and the involvement of the N-H groups. The strongest interaction is found in the presence of Primaquine followed by Chloroquine and Quinine. But we need another technique to gain more insights into the strength of these interactions.

3.5.2. Thermogravimetric Analysis and DSC

To gain more insight into the thermal stability of the association of aurein and antimalarials, Thermogravimetric Analysis (TGA) and Differential Scanning Calorimetry (DSC) were used [34] [35].

1) TGA

The results of the thermogravimetric curves of aurein and its complexes of antimalarials are summarized in Table 16. The weight losses obtained from all the samples are given in percentages. According to the literature, the weight loss points around 25˚C - 300˚C correspond to the loss of water. The weight loss point around 300˚C - 400˚C corresponds to the decomposition of aurein and its complexes. Aurein loses 5.41% of its mass between 25˚C and 100˚C, 6.89% of its mass in the 100˚C - 200˚C range, and 31.2% of its mass between 200˚C and 300˚C. There is a total of about 43.5% of its content in water. Another loss of mass occurs after 300˚C, corresponding to the decomposition of the peptide. A comparison of the weight loss of the pure antimalarials and pure aurein reveals that aurein contains more water than the pure antimalarials; however, in the range between 25˚C - 100˚C, the pure antimalarials and the aurein/antimalarial

complexes lose more mass than aurein. This result suggests that aurein is very stable over the 25˚C - 100˚C temperature range. In the range 25˚C - 400˚C, aurein is definitively more stable than Chloroquine, as aurein loses 67.7% of its mass and Chloroquine loses 70.67% of its mass. Quinine and Primaquine are more stable than aurein Table 16. Aurein destabilizes Quinine with 61.53% mass loss for aurein-Quinine against 50.05% mass loss for Quinine alone. Aurein stabilizes Primaquine with 48.54% mass loss for aurein-Primaquine against 50.72% mass loss for Primaquine alone. Aurein stabilizes Chloroquine with 66.85% mass loss for aurein-Chloroquine against 70.67% mass loss for Chloroquine alone.

In the range 25˚C - 400˚C, Quinine and Primaquine are more stable than aurein and Chloroquine. When considering the complexes of antimalarials with aurein, the most stable association is aurein-Primaquine with 48.54% mass loss.

2) DSC

The DSC results of the thermogram curves of aurein and its complexes are summarized in Table 17. The enthalpy values are given in joules per gram (J/g) [33] [34] [35].

The DSC thermogram curves of aurein, Quinine, are presented in Figure 11 and Figure 12, respectively. Figure 11 displays the thermogram curve of aurein. The DSC thermogram is characterized by three broad endothermic peaks between 25˚C and 700˚C. The first endothermic peak between 25˚C and around 270˚C can be attributed to bound water. The second and third endothermic peaks between 270˚C and 700˚C can be attributed to the breaking of the peptide bonds (second peak) followed by decarboxylation from the breaking of the peptide bonds (third peak). The broadness of the peaks is characteristic of the complexity of the transitions that include disruption of peptide-water interactions, evaporation and vaporization. The characteristic parameters of such a transition are reported in Table 17. The enthalpy of the transition (ΔH) corresponds to the area under the curve.

To gain insights into the stability of the association aurein and antimalarials, we use the enthalpy values Table 18. In the 25˚C - 700˚C range, 5495.7 J/g of energy is required to break aurein. Quinine requires 9361.48 J/g to be broken, and Primaquine and Chloroquine requires less energy to be broken. These high

Table 17. Mass Percent Loss of aurein and its complexes over the 25˚C - 400˚C temperature range.

	Mass loss (%)						
Temperature range (˚C)	Aurein	Quinine	Aurein-Quinine	Primaquin	Aurein-Prima	Chloroquin	Aurein-Chloro
25 - 100	5.41	16.2	10.5	7.12	8.75	9.07	11
101 - 200	6.89	5.46	6.53	16.7	6.99	18.5	6.55
201 - 300	31.2	8.19	23	16.3	19.8	16.9	28.9
301 - 400	24.2	20.2	21.5	10.6	13	26.2	20.4
Total mass loss (%)	67.7	50.05	61.53	50.72	48.54	70.67	66.85

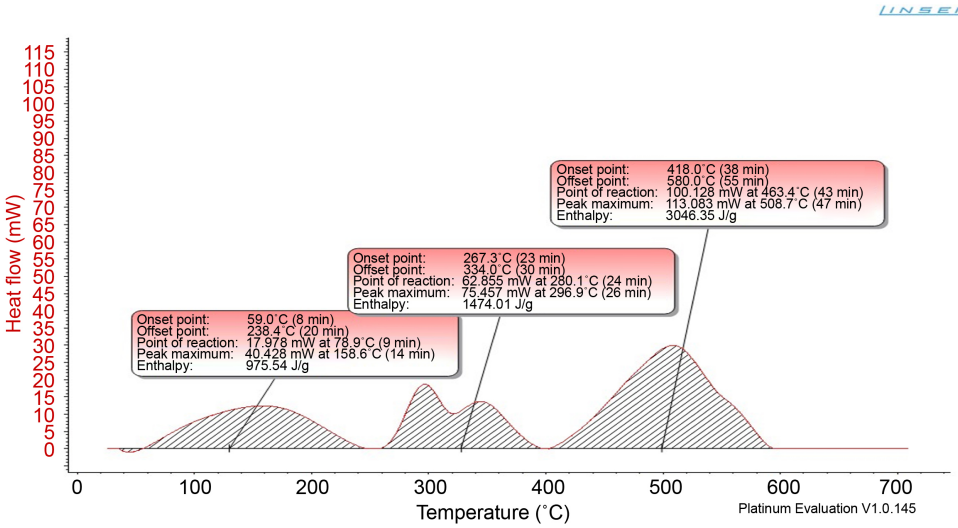

Figure 11. DSC thermogram of aurein.

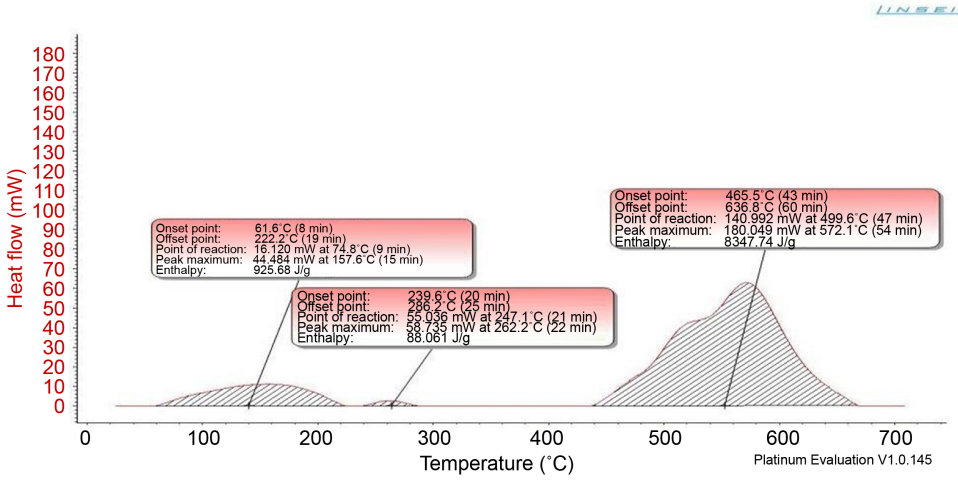

Figure12. DSC thermogram of Quinine.

Table 18. DSC thermograms of aurein and its complexes with antimalarials.

Sample name	Temperature range (˚C)	Enthaly (J/g) to remove water	Temperature range (˚C)	Enthaly (J/g) to break the sample	Total Enthaly (25˚C - 700˚C) (J/g)
Aurein	25 - 300	975.34	300 - 700	4520.36	5495.7
Quinine	25 - 300	1013.74	300 - 700	8347.74	9361.48
Aurein-Quinine	25 - 300	456.23	300 - 700	8702.62	9158.85
Primaquine	25 - 300	165.41	300 - 700	1165.11	1330.52
Aurein-Primaquine	25 - 300	825.9	300 - 700	1769.75	2595.65
Chioroquine	25 - 300	449.44	300 - 700	1401.85	1851.29
Aurein-Chioroquine	25 - 350	375.32	300 - 700	2123.14	2498.46

enthalpy values mean that Quinine and aurein are very stable compounds, but Quinine is more stable, because its enthalpy value is almost twice that of aurein.

The addition of aurein to Quinine decreases the value of the enthalpy of Quinine while increasing that of aurein. The results suggest that the complex aurein-Quinine is relatively stable. The addition of aurein to Primaquine or Chloroquine increases the value of the enthalpy of Primaquine or Chloroquine while decreasing that of aurein. The results suggest that the complex aurein-Primaquine and aurein-Chloroquine are also stable but the mechanism of interaction between aurein and the three antimalarials are different, as already suggested but infrared and fluorescence results. The aurein-primquine may be more stable than aurein-Chloroquine because the increase of the enthalpy value of primquine is almost doubled in the presence of aurein, and this result agrees with the TGA result. Aurein and Quinine are very stable compounds but the aurein-Primaquine complex seems to be the most stable. In pharmaceutical terms, the probability of drugdrug interaction between aurein and Primaquine is very high, which means avoiding Primaquine while taking aurein is recommended. Quinine may be administered after a few hours.

4. Conclusion

The interactions of the effective antimicrobial peptide aurein with various model membranes of different lipid compositions have been investigated. FTIR studies gave insights on the secondary structural changes that the peptide undergoes in the presence of the membrane as well as an understanding of conformational changes occurring to the lipids composing the membranes. These results were verified through the use of TGA/DSC techniques, which corroborated that there was no interference present in from water in the amide I region of the FTIR spectra. The stability measured by TGA/DSC was indicative of cellular disruption and destabilization through lipid-peptide interactions.

Conflicts of Interest

The authors declare no conflicts of interest regarding the publication of this paper.

References

[1] López-Meza, J.E., Ochoa-Zarzosa, A., Barboza-Corona, J.E. and Bideshi, D.K. (2015) Antimicrobial Peptides: Current and Potential Applications in Biomedical Therapies. *BioMed Research International*, **2015**, Article ID: 367243. https://doi.org/10.1155/2015/367243

[2] Collignon, P.J. (2002) Antibiotic Resistance. *Medical Journal of Australia*, **177**, 325-329. https://doi.org/10.5694/j.1326-5377.2002.tb04794.x

[3] World Health Organization (2014) Antimicrobial Resistance: Global Report on Surveillance. http://www.who.int/drugresistance/documents/surveillancereport/en/

[4] Reddy, K.V., Yedery, R.D. and Arana, C. (2004) Antimicrobial Peptides: Premises and Promises. *International Journal of Antimicrobial Agents*, **24**, 536-547. https://doi.org/10.1016/j.ijantimicag.2004.09.005

[5] Yeaman, M.R. and Yount, N.Y. (2003) Mechanisms of Antimicrobial Peptide Ac-

tion and Resistance. *Pharmacological Review*, **55**, 27-55. https://doi.org/10.1124/pr.55.1.2

[6] Sevcsik, E., Pabst, G., Richter, W., Danner, S., Amenitsch, H. and Lohner, K. (2008) Interaction of LL-37 with Model Membrane Systems of Different Complexity: Influence of the Lipid Matrix. *Biophysical Journal*, **94**, 4688-4699. https://doi.org/10.1529/biophysj.107.123620

[7] Sitaram, N., Subbalashmi, C. and Nagaraj, R. (2003) Indolicidin, a 13-Residue Basic Antimicrobial Peptide Rich in Tryptophan and Proline, Interacts with Ca^{2+}-Calmodulin. *Biochemical and Biophysical Research Communications*, **309**, 879-884. https://doi.org/10.1016/j.bbrc.2003.08.095

[8] Subbalakshmi, C. and Sitaram, N. (1998) Mechanism of Antimicrobial Action of Indolicidin. *FEMS Microbiology Letter*, **160**, 91-96. https://doi.org/10.1016/S0378-1097(98)00008-1

[9] Rozek, A., Friedrich, C.L. and Hancock, R.E. (2000) Structure of the Bovine Antimicrobial Peptide Aurein Bound to Dodecylphophocholine and Sodium Dodecyl Sulfate Micelles. *Biochemistry*, **39**, 15765-15774. https://doi.org/10.1021/bi000714m

[10] Rozek, T., *et al*. (2000) The Antibiotic and Anticancer Active Aurein Peptides from the Australian Bell Frogs *Litoria aurea* and *Litoria raniformis*. *European Journal of Biochemistry*, **267**, 5330-5341. https://doi.org/10.1046/j.1432-1327.2000.01536.x

[11] Zhao, L. and Feng, S. (2004) Effects of Lipid Chain Length on Molecular Interactions between Paclitaxel and Phospholipid within Model Biomembranes. *Journal of Colloid and Interface Science*, **274**, 55-68. https://doi.org/10.1016/j.jcis.2003.12.009

[12] Zhang, T., Muraih, J.K., Tishbi, N., Herskowitz, J., Victor, R.L., Silverman, J., Mintzer, E., *et al*. (2014) Cardiolipin Prevents Membrane Translocation and Permeabilization by Daptomycin. *Journal of Biological Chemistry*, **289**, 11584-11591. https://doi.org/10.1074/jbc.M114.554444

[13] Goluszko, P. and Nowicki, B. (2005) Membrane Cholesterol: A Crucial Molecule Affecting Interactions of Microbial Pathogens with Mammalian Cells. *Infection and Immunity*, **73**, 7791-7796. https://doi.org/10.1128/IAI.73.12.7791-7796.2005

[14] Hancock, R.E.W. and Rozek, A. (2002) Role of Membranes in the Activities of Antimicrobial Cationic Peptides. *FEMS Microbiology Letters*, **206**, 143-149. https://doi.org/10.1111/j.1574-6968.2002.tb11000.x

[15] McHenry, A.J., Sciacca, M.F.M., Brender, J.R. and Ramamoorthy, A. (2012) Does Cholesterol Suppress the Antimicrobial Peptide Induced Disruption of Lipid Raft Containing Membranes? *Biochimica et Biophysica Acta* (*BBA*)—*Biomembranes*, **1818**, 3019-3024. https://doi.org/10.1016/j.bbamem.2012.07.021

[16] Beriashvili, D., Taylor, R., Kralt, B., Abu Mazen, N., Taylor, S.D. and Palmer, M. (2018) Mechanistic Studies on the Effect of Membrane Lipid Acyl Chain Composition on Daptomycin Pore Formation. *Chemistry and Physics of Lipids*, **216**, 73-79. https://doi.org/10.1016/j.chemphyslip.2018.09.015

[17] Der Laarse, A.V., Höld, K.M. and Bastiaanse, E.L. (1997) The Effect of Membrane Cholesterol Content on Ion Transport Processes in Plasma Membranes. *Cardiovascular Research*, **33**, 272-283. https://doi.org/10.1016/S0008-6363(96)00193-9

[18] Mills, T., Huang, J., Feigenson, G. and Nagle, J. (2009) Effects of Cholesterol and Unsaturated DOPC Lipid on Chain Packing of Saturated Gel-Phase DPPC Bilayers. *General Physiology and Biophysics*, **28**, 126-139. https://doi.org/10.4149/gpb_2009_02_126

[19] Cheng, J.T.J., Hale, J.D., Elliot, M., Hancock, R.E.W. and Straus, S.K. (2011) The Importance of Bacterial Membrane Composition in the Structure and Function of

Aurein 2.2 and Selected Variants. *Biochimica et Biophysica Acta* (*BBA*)—*Biomembranes*, **1808**, 622-633. https://doi.org/10.1016/j.bbamem.2010.11.025

[20] Echelon Biosciences (2015) Product Details for 1, 2-Dioleoyl-sn-Glycero-3-Phosphocholine (DOPC) [4235-95-4]: Assay and Reageants for Drug Discovery in Lipid Signaling Pathways. https://www.echelon-inc.com/product/dlpc-120-pc/

[21] Freed, J.H. and Ge, M. (2003) Hydration, Structure, and Molecular Interactions in the Headgroup Region of Dioleoylphosphatidylcholine Bilayers: An Electron Spin Resonance Study. *Biophysical Journal*, **85**, 4023-4040. https://doi.org/10.1016/S0006-3495(03)74816-4

[22] Csiszár, A., Koglin, E., Meier, R.J. and Klumpp, E. (2006) The Phase Transition Behavior of 1,2-Dipalmitoyl-Sn-Glycero-3-Phosphocholine (DPPC) Model Membrane Influenced by 2,4-Dichlorophenol—An FT-Raman Spectroscopy Study. *Chemistry and Physics of Lipids*, **139**, 115-124. https://doi.org/10.1016/j.chemphyslip.2005.11.005

[23] Chan, Y.H.M. and Boxer, S.G. (2007) Model Membrane Systems and Their Applications. *Current Opinion in Chemical Biology*, **11**, 581-587. https://doi.org/10.1016/j.cbpa.2007.09.020

[24] Sitaram, N. and Nagaraj, R. (1999) Interaction of Antimicrobial Peptides with Biological and Model Membranes: Structural and Charge Requirements for Activity. *Biochimica et Biophysica Acta* (*BBA*)—*Biomembranes*, **1462**, 29-54. https://doi.org/10.1016/S0005-2736(99)00199-6

[25] Center for Strategic and International Studies (2015) Infectious Diseases: A Persistent Threat. http://www.smartglobalhealth.org/issues/entry/infectious-diseases

[26] American Chemical Society International Historic Landmarks (2014) Discovery and Development of Penicillin. http://www.acs.org/content/acs/en/education/whatischemistry/landmarks/flemingpenicillin.html

[27] Viola, G., Salvador, A., Cecconet, L., Basso, G., Vedaldi, D., Dall'Acqua, F., Aloisi, G.G., Amelia, M., Barbafina, A., Latterini, L. and Elisei, F. (2007) Photophysical Properties and Photobiological Behavior of Amodiaquine, Primaquine and Chloroquine. *Photochemistry and Photobiology*, **83**, 1415-1427. https://doi.org/10.1111/j.1751-1097.2007.00181.x

[28] Dyck, M., Kerth, A., Blume, A. and Losche, M. (2006) Interaction of the Neurotransmitter, Neuropeptide Y, with Phospholipid Membranes: Infrared Spectroscopic Characterization at the Air/Water Interface. *The Journal of Physical Chemistry B*, **110**, 22152-22159. https://doi.org/10.1021/jp062537q

[29] Blume, A., Hubner, W. and Messner, G. (1988) Fourier Transform Infrared Spectroscopy of 13C: O-Labeled Phospholipids Hydrogen Bonding to Carbonyl Groups. *Biochemistry*, **27**, 8239-8249. https://doi.org/10.1021/bi00421a038

[30] Grdadolnik, J. and Hadzi, D. (1998) FT Infrared and Raman Investigation of Saccharide-Phosphatidylcholine Interactions Using Novel Structure Probes. *Spectrochimica Acta Part A*: *Molecular and Biomolecular Spectroscopy*, **54**, 1989-2000. https://doi.org/10.1016/S1386-1425(98)00111-5

[31] Giovanela, M., Parlanti, E., Soriano-Sierra, E.J., Sold, M.S. and Sierra, M.M.D. (2004) Elemental Compositions, FT-IR Spectra and Thermal Behavior of Sedimentary Fulvic and Humic Acids from Aquatic and Terrestrial Environments. *Geochemical Journal*, **38**, 255-264. https://doi.org/10.2343/geochemj.38.255

[32] Samouillan, V., Dandurand-Lods, J., lamure, A., Maurel, E., Lacabanne, C., Gerosa, G., Vanturini, A., Casarotto, D., Gheraldini, L. and Spina, M. (1999) Thermal Anal-

ysis Characterization of Aortic Tissues for Cardiac Valves Bioprostheses. *Journal of Biomedical Materials Research*, **46**, 531-538. https://doi.org/10.1002/(SICI)1097-4636(19990915)46:4<531::AID-JBM11>3.0.CO;2-2

[33] Morel, B., Varela, L. and Conejero-Lara, F. (2010) The Thermodynamic Stability of Amyloid Fibrils Studied by Differential Scanning Calorimetry. *The Journal of Physical Chemistry B*, **114**, 4010-4019. https://doi.org/10.1021/jp9102993

[34] Akkara, J.A., Senegal, K.J. and Kaplan, D.L. (1991) Synthesis and Characterization of Polymers Produced by Horseradish in Dioxane. *Journal of Polymer Science*: *Part A*: *Polymer Chemistry*, **29**, 1561-1574. https://doi.org/10.1002/pola.1991.080291105

[35] Kaasgaard, T., Mouritsen, O.G. and Jorgensen, K. (2003) Freeze/Thaw Effects on Lipid-Bilayer Vesicles Investigated by Differential Scanning Calorimetry. *Biochimica et Biophysica Acta* (*BBA*)—*Biomembranes*, **1615**, 77-85. https://doi.org/10.1016/S0005-2736(03)00194-9

[36] Russell, A.L., Kennedy, A.M., Spuches, A.M., Gibson, W.S., Venugopal, D., Klapper, D., Srouji, A.H., Bhonsle, J.B. and Hicks, R.P. (2011) Determining the Effect of the Incorporation of Unnatural Amino Acids into Antimicrobial Peptides on the Interactions with Zwitterioninc and Anionic Membrane Model Systems. *Chemistry and Physics of Lipids*, **164**, 740-758. https://doi.org/10.1016/j.chemphyslip.2011.09.003

[37] Liyanage, M.R., Bakshi, K., Volkin, D.B. and Middaugh, C.R. (2013) Fluorescence Spectroscopy of Peptides. In: Nixon, A., Ed., *Therapeutic Peptides*, Humana Press, Totowa, 237-246. https://doi.org/10.1007/978-1-62703-673-3_16

[38] Ahn, J.J., Kim, Y., Lee, S.Y., Hong, J.Y., Kim, G.W. and Hwang, S.Y. (2015) Fluorescence Melting Curve Analysis Using Self-Quenching Duallabeled Peptide Nucleic Acid Probes for Simultaneously Identifying Multiple DNA Sequences. *Analytical Biochemistry*, **484**, 143-147. https://doi.org/10.1016/j.ab.2015.05.022

[39] Aoki, W., Kitahara, N., Fujita, A., Shibasaki, S., Morisaka, H., Kuroda, K. and Ueda, M. (2013) Detection of *Candida albicans* by Using a Designed Fluorescence-Quenched Peptide. *Journal of Bioscience and Bioengineering*, **116**, 573-575. https://doi.org/10.1016/j.jbiosc.2013.05.003

[40] Zamotaiev, O.M., Postupalenko, V.Y., Shvadchak, V.V., Pivovarenko, V.G., Klymchenko, A.S. and Mely, Y. (2011) Improved Hydrationsensitive Dual-Fluorescence Label for Monitoring Peptide-Nucleic Acid Interactions. *Bioconjugate Chemistry*, **22**, 101-107. https://doi.org/10.1021/bc100434d

[41] Shaw, J., Slade, A. and Yip, C. (2003) Simultaneous *in Situ* Total Internal Reflectance Fluorescence/Atomic Force Microscopy Studies of DPPC/dPOPC Microdomains in Supported Planar Lipid Bilayers. *Journal of the American Chemical Society*, **125**, 11838-11839. https://doi.org/10.1021/ja0370894

[42] Eastman, T. (1996) Adhesion Forces between Surface-Modified AFM Tips and a Mica Surface. *Langmuir*, **12**, 2859-2862. https://doi.org/10.1021/la9504220

[43] Santos, N.C. and Castanho, M. (2004) An Overview of the Biophysical Applications of Atomic Force Microscopy. *Biophysical Chemistry*, **107**, 133-149. https://doi.org/10.1016/j.bpc.2003.09.001

[44] McDuffee, A.T., Senisterra, G., Huntley, S., Lepock, J.R., Sekhar, K.R., Meredith, M.J., Borrelli, M.J., Morrow, J.D. and Freeman, M. (1997) Proteins Containing Non-Native Disulfide Bonds Generated by Oxidative Stress Can Act as Signals for the Induction of the Heat Shock Response. *Journal of Cellular Physiology*, **171**, 143-151. https://doi.org/10.1002/(SICI)1097-4652(199705)171:2<143::AID-JCP4>3.0.CO;2-O

[45] Dundurand, J., Samouillan, V., Lacoste-Ferre, M.H. and Lacabanne, C. (2014) Con-

formational and Thermal Characterization of a Synthetic Peptidic Fragment Inspired from Human Tropoelastin: Signature of the Amyloid Fibers. *Pathologie Biologie*, **62**, 100-107. https://doi.org/10.1016/j.patbio.2014.02.001

[46] Kimura, S., Yamashita, S. and Okamoto, T. (1986) Differential Scanning Calorimetry of Lipids of Stored Apples. *Agricultural and Biological Chemistry*, **50**, 707-711. https://doi.org/10.1080/00021369.1986.10867444

[47] Hirata, I.Y., Cezari, M.H.S., Juliano, M.A. and Juliano, L. (1995) Internally Quenched Fluorogenic Protease Substrates: Solid-Phase Synthesis and Fluorescence Spectroscopy of Peptides Containing Ortho-Aminobenzoyl/Dinitrophenyl Groups as Donor-Acceptor Pairs. *Letters in Peptide Science*, **1**, 299-308. https://doi.org/10.1007/BF00119771

[48] Wittenburg, S., Stankewicz, C. and Rininsland, F. (2006) Biotinylated Peptides for Rapid Identification of Substrates and Inhibitors of Kinases and Phosphatases with Fluorescence Superquenching. *Assay and Drug Development Technologies*, **4**, 535-543. https://doi.org/10.1089/adt.2006.4.535

[49] Pinheiro, M., Arede, M., Giner-Casares, J.J., Nunes, C., Caio, J.M., Moiteiro, C., Lucio, M., Camacho, L. and Reis, S. (2013) Effects of a Novel Antimycobacterial Compound on the Biophysical Properties of a Pulmonary Surfactant Model Membrane. *International Journal of Pharmaceutics*, **450**, 268-277. https://doi.org/10.1016/j.ijpharm.2013.03.062